Damage evaluation by means of cyclostationarity

D.Boungou [1,2]**, P. Lyonnet** [1] **, F.Guillet** [2] **, R.Toscano** [1]**, M. El-Badaoui** [2]
[1] LTDS, Ecole National d'Ingnieurs de St-etienne
St-tienne
e-mail: **darcy.boungou@univ-st-etienne.fr**

[2] LASPI, Universit Jean-Monnet
Roanne

Abstract
Our study focuses on the estimation of 316L stainless steel specimens lifetime, subjected to Low Cycle Fatigue (LCF) and High Cycle Fatigue (HCF). So we developed a fatigue damage test rig using alternative bending. The LCF is defined by repetitive cyclic stress in a short period. The material behaviour subjected to LCF and HCF can provide information linked to the fatigue damage. The purpose of this study is to analyze and caracterize the fatigue of a material subjected to LCF and HCF using signal processing tools. We observe that the specimen vibration signal is a coupling of periodic phenomenon (cycle of sollicitaion) with random stationary phenomenon (random amplitude due to the fatigue damage). For this reason spectral analysis and cyclostationary study are carry out during the manipulation setup. Our observations show that the fatigue damage of the material produces a periodic stochastic processes (cyclostationarity of order 2) appear in vibration signal. Accordingly we propose a new indicator for fatigue damage : the amplitude of cyclic frequencies.

1 Introduction

The fatigue damage is one of the main causes of machines defect found in industry. The detection of this type of damage is very difficult and this affects the maintenance scheduling. To estimate machines lifetime which are subjected to fatigue damage, the reliability is the most frequently used. In fact, the using of data bases as input for reliability measurment will not always give reliable results. Therefore, other machines lifetime estimation methods have been investigated to propose damage indicators and estimate lifetime corresponding. Thereby, we use the signal processing approach to suggest a new damage indicator.

Our study focuses on the estimation of the lifetime of 316L stainless steel specimens subjected to LCF and HCF. To carry out our study, a fatigue damage test rig using alternative bending is manipulated. The material behaviour subjected to LCF or HCF can present information linked to the fatigue damage, and the study of the specimen vibration signal can provide an indication about the fatigue damage state. In the framework of signal processing, a study has shown that the cyclostationary analysis of vibration signal of foot ground reaction forces provides the identification and evaluation of gait and running abnormalities. [1] show that the cyclostationarity provide information about the development of runner's fatigue .

Cyclostationarity is a property that characterizes stochastic processes whose statistical properties periodically vary with time. An important amount of work has been achieved since then, especially by Gardner et al. [2][3], yet it is only during the last two decades that cyclostationarity has led to important breakthroughs in communications and breached the usual assumption of stationary [4].

This paper is organized as follows : In the section 1 we present the test rig and the acquisition system. In the section 2 we analyze and characterize the collected signals. A brief review of cyclostationary analysis and

its basic concept is exhibited in the section 3. In the section 4 we identify and quantify the specimen fatigue damage and by means of cyclostationarity and make a matching with materials technology. It demonstrates that the fatigue damage of the material produces a cyclostationarity of order 2 in the vibration signal. To finish we propose the Energy of the Cyclic Frequency (ECF) as a new fatigue damage indicator.

2 Test rig description

The test rig consists of differents parts :

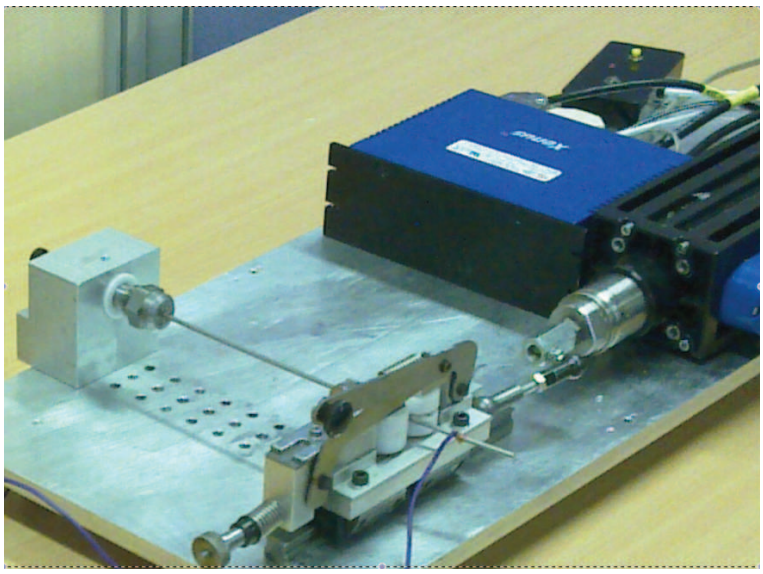

Figure 1: Test rig

- Test specimen : 316L stainless steel,
- Linear motor and variable-speed drive,
- Bending dispositif,
- Data acquisition system.

A linear motor is controlled by a variable-speed drive. With a bending device, one-sidedly clamped specimen is bent by the motor movement. This cyclic deformation provides alternative bending of the test specimen and under many cycles, the specimen gets damaged by fatigue and breaks.

2.1 The test specimen : 316L stainless steel

The studied material is an austenitic chromium- nickel stainless steel containing molybdenum Z2CND17-12 (AISI 316L). This addition increases general corrosion resistance, improves resistance to pitting from chloride ion solutions, and provides increased strength at elevated temperatures.The experimentation is carried out on a specimen of 3mm diameter at differents lengths : 200mm ; 245mm ,corresponding to different stress.

Figure 2: Stainless less 316L

Physical Properties 316L Stainless Steel	
Density	8000 Kg/m^3
Elastic Modulus	193 GPa
Tensile Strength, Yield R_p 0.2%	220 MPa
Breaking loads	520-670 MPa
Mean co-eff of Therma expansion $0 - 100^0C$	15.9 $\mu m/m/^0C$
Thermal Conductivity at 100^0C	16.3 $W/m.K$
Specific Heat $0 - 100^0C$	500 $J/kg.K$)
Elec Resistivity	740 $n\Omega.m$

2.2 The linear motor and the variable-speed drive

Comprising just two parts, a rod and forcer, the tubular linear motor Figure(3) is inherently simple . The stainless steel rod is filled with magnets placed end to end. The forcer incorporates a series of coils connected as three phase windings. When the coils are excited by three phase current, a magnetic field is created and interacts with the rod magnetic field, generating linear force.

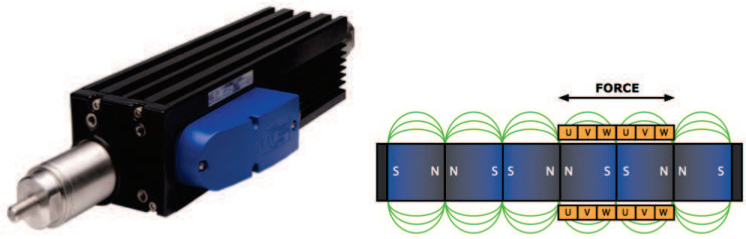

Figure 3: The tubular linear motor and magnetization system

The variable-speed drive Figure(4) is in reality an automaton device. It is used to load instructions to the operating motor: the movement type, amplitude and frequency etc. These instructions are notified in a special software of monitoring CME2.

The software CME2 is provided with the variable-speed drive, it allows to monitoring the motor in applying instructions through the variable-speed. The documentation $CME2_{U}sr_{G}uide$ gives many information about its utility. After setting the software (active port, motor type, units, etc.), when it operates, the following window Figure(5) appears. In pressing in 'CVM Control Program' the machine virtual screen is opened in which instructions are entered. The communication with the computer is done through RS232 connexion, that recieves orders in ASCII language.

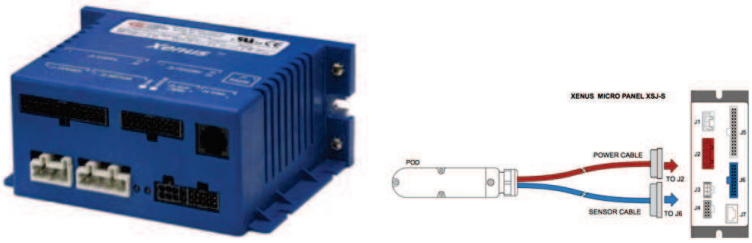

Figure 4: Variable-speed drive and its connections to the motor

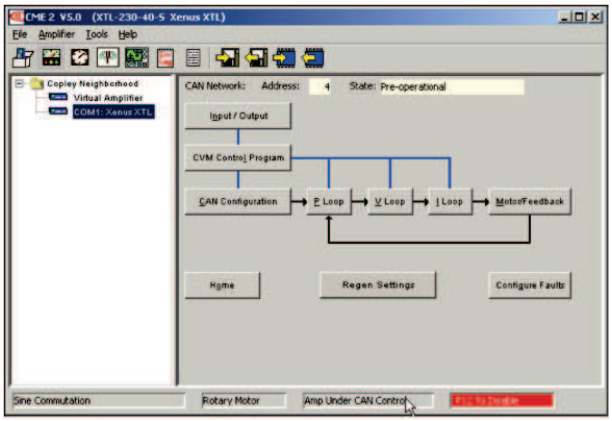

Figure 5: CME2 Software

2.3 The bending device

The bending device figure(6) is a kind of mechanical system, designed exclusively for this test bench. It is mainly constituted of 4 functional elements :

- (1) 2 ceramic rollers that bend the test specimen during the linear motor movement. So during the test, the test specimen is smoothly bended due to the turning rollers around themselves. Ceramic is a good insulator, with a good friction coefficient and heat dissipation.

- (2) a spacer system of ceramic rollers held by a spring. It allows placing and holding in position the test specimen.

- (3) a horizontal clamping screw, regulates the space between the ceramic rollers.

- (4) a linear guide rail moves the set (1) (2) and (3) relative to the frame.

2.4 The fixing system

The specimen holding is adjusted with device presented in figure(7). The system consists of three parts attached via specimen. These parts are :

- (1) The fixing block to the frame,

- (2) The threaded steel tube ,

- (3) The set that holds one specimen end in position.

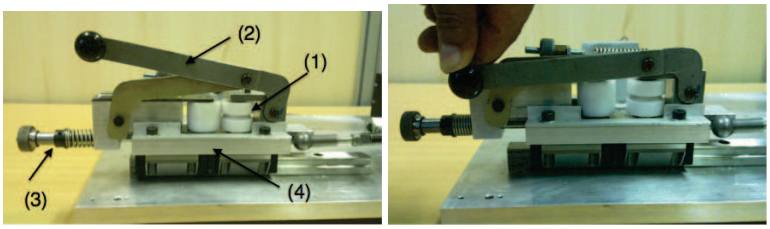

Figure 6: System bending

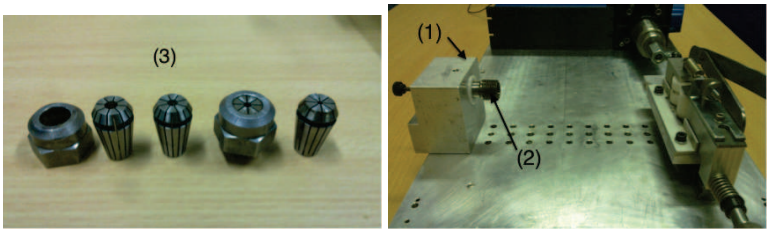

Figure 7: System fixing

2.5 The data acquisition system

To record vibration signal we used the National Instrument PCI-4462 24-bit. It is a high-accuracy data acquisition board specifically designed for sound and vibration applications. The NI PCI-4462 features 118 dB dynamic range and six gain settings for precision measurements with microphones, accelerometers, and other transducers that operate at high dynamic ranges. To count the number of cycles of motor and record automatically the specimen vibration signal, we designed a specific application in LabVIEW language. Labview is a National Instruments system design software that provides to create and deploy measurement and control systems through unprecedented hardware integration figure(8).

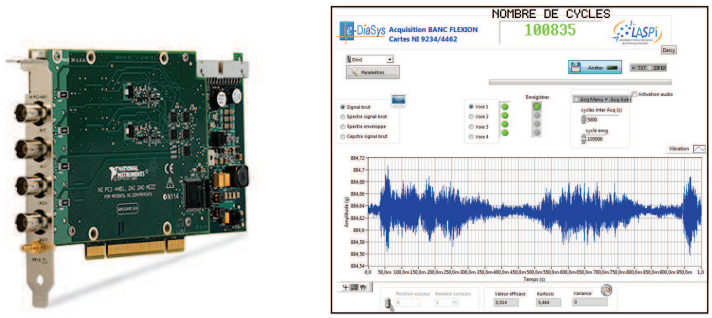

Figure 8: NI PCI-4462 and Acquisition software

3 Analysis and characterization of signals

The vibration signal is sampled in 50 Khz and recorded every 1000 cycles until the specimen breaks. A cycle is defined as a double bending of a specimen during the linear motor's translation. At low temperature (room temperature), the mechanical cyclic stress creates external stress field which shifts the metallic crystals. These dislocations lead sliding in intra-granules, allowing elastic or plastic deformation amplitude d [5], [6].

This sliding correspond to the link fracture between atoms, producing free electrons as showed in figure (9).

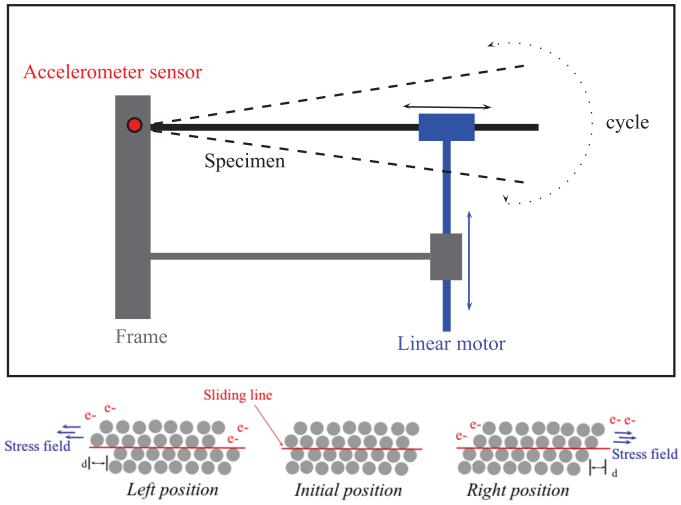

Figure 9: Intra-granules sliding

This link fracture between atoms appears in the vibration signal as periodic burts with period $T_0/2 = 1/2f_0$ corresponding to each bend. A cycle is defined for a periode $T_0 = 1/f_0$.

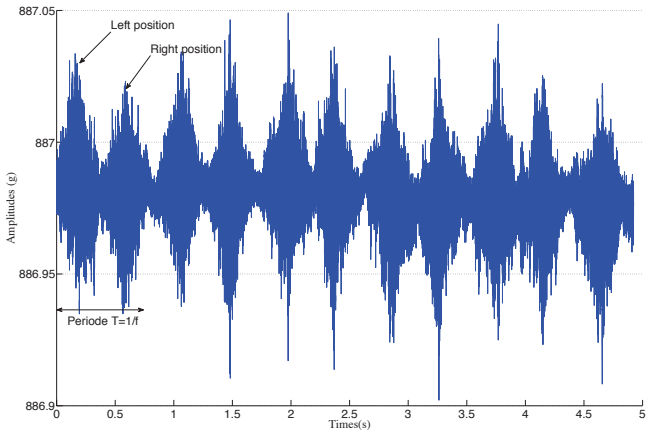

Figure 10: Vibration signal

4 Cyclostationary analysis

4.1 Basic definitions

A signal is cyclostationary when its statistical moments are periodic.This type of signal can be define as stochastic process that exhibits some hidden periodicity of its energy flow. In mechanical systems under constant operating (speed, torque...) this hidden periodicity is due to the various rotation of mechanical components which produce periodic modulations of the vibration signal [4].

To depict how the energy relative to the hidden periodicity travels with time, the idea is to decompose the energy flow into pediodic component. For that, let us introduce an extraction operator $\mathscr{P}$ that extracts all

periodic components contained in a time function :

$$\mathscr{P}\{.\} = \sum_{\alpha \in \mathscr{A}} \left(\lim_{T \to \infty} \frac{1}{T} \int_T (.)\, e^{-j2\pi\alpha t} dt \right) .e^{j2\pi\alpha t} \tag{1}$$

$\mathscr{A}$ is the set containing all cyclic frequencies α associed with non-zero periodic component, $\int_T (.)\, dt$ means the summation over an interval of length T, frequencies α are commonly known as *the cyclic frequencies* of the signal, and its inverse as cycles. Let us denote $\mathscr{P}_0\{.\}$ to be on operator corresponding to $\mathscr{P}$ when $\alpha = 0$ (in the case of stationary random signal), this operator extract the time-average value (DC component) of a signal:

$$\mathscr{P}_0\{.\} = \lim_{T \to \infty} \frac{1}{T} \int_T (.)\, dt \tag{2}$$

The Fourier Transform of $x(t)$ is given by :

$$\mathscr{P}_0\{x(t).e^{-j2\pi\alpha t}\} = \lim_{T \to \infty} \frac{1}{T} \int_T x(t) e^{-j2\pi\alpha t} dt. \tag{3}$$

After defining these operators, let us introduce more advanced signal processing tools.

4.2 Orders of cyclostationarity

A cyclostationary signal can be decomposed as a mean value part $m_x(t) = \mathscr{P}\{x(t)\}$ and residual part $\mathscr{R}\{x(t)\}$:

$$x(t) = \mathscr{P}\{x(t)\} + \mathscr{R}\{x(t)\} \tag{4}$$

Where $\mathscr{P}\{x(t)\}$ includes all the periodic components of the signal, it is the *deterministic part* . The residual part $\mathscr{R}\{x(t)\}$ includes all the random components that exhibits some hidden periodicity of its energy flow, it is the *random part* . The introduced decomposition, remind that a signal is cyclostationary when its statisticals moments are periodic. Let's give precisions about orders of cyclostationarity :

- A signal is said to be purely *cyclostaionary at order 1* , ie $\mathscr{P}\{x(t)\} = \mathscr{P}\{x(t + T_0)\}$ with T_0 the period of the signal, if its residual part $\mathscr{R}\{x(t)\}$ does not exhibit cyclostationarity at any order.
- A signal is said to be purely *cycloastationary at order 2* if its derterministic part $\mathscr{P}\{x(t)\}$ is nil and its residual part $\mathscr{R}\{x(t)\}$is cyclostationarity at order 2, ie there exists a value of τ for which the interaction $x(t + \tau/2)x(t - \tau/2)$ produces a periodic component :$R_x(t, \tau) = R_x(t + T, \tau + T)$ with $T = 1/\alpha$ the cyclic period, where $R_x(t, \tau)$ is the autocorrelation function.

It is rarely that mechanical systems produces signals that are purely cyclostationary at a given order, they are rather a combination of several orders of cyclostationariy.

4.3 Estimation of the deterministe part

The $\mathscr{P}$-operator applied to the cyclostationary signal $x(t)$ extracts the signal *synchronous average* $m_x(t)$, with period T and number of period K:

$$\begin{aligned} m_x(t) &= \mathbb{E}\{x(t + nT)\} = \mathscr{P}\{x(t)\} \\ &= \sum_{\alpha \in \mathscr{A}} \mathscr{P}_0\{x(t).e^{-j2\pi\alpha t}\}.e^{j2\pi\alpha t} \\ &= \sum_{\alpha \in \mathscr{A}} M_x^\alpha .e^{j2\pi\alpha t} \end{aligned} \tag{5}$$

The quantities M_x^α are the non-zero coefficients decomposotion Fourier with. $m_x(t)$ can be estimated as follows, figure (11):

$$m_x(t) = \frac{1}{K}\sum_{n=0}^{K-1} x(t+nT) \tag{6}$$

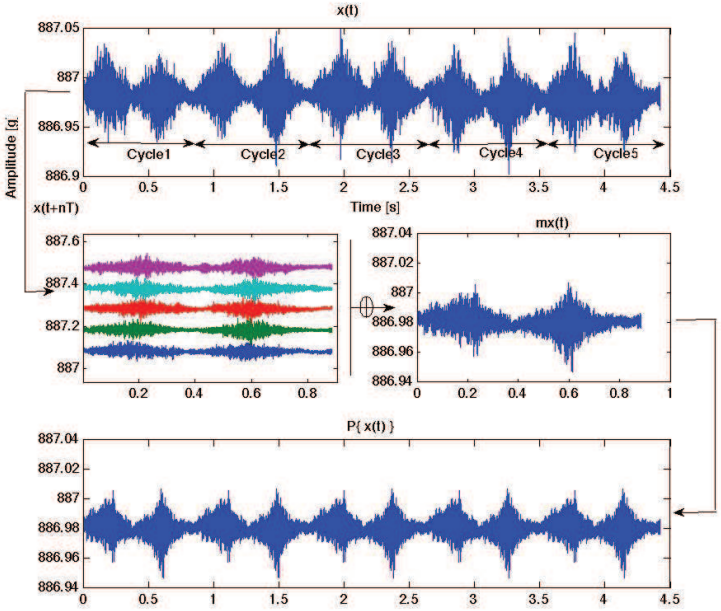

Figure 11: Principle of the time synchronous average illustrated on a vibration signal

4.4 Estimation of cyclostationarity at order 2

The first step is to extract the predictable part $\mathscr{P}\{x(t)\}$ from the signal $x(t) : \mathscr{R}\{x(t)\} = x(t) - \mathscr{P}\{x(t)\}$.

Figure (12) displays the vibration signal over 5 cycles together with its decomposition into a mean value $\mathscr{P}\{x(t)\}$ and a residuel value $\mathscr{R}\{x(t)\}$. We observe a strong periodic mean value in $\mathscr{P}\{x(t)\}$ synchronised on the engine cycle. It is noteworthy that $\mathscr{P}\{x(t)\}$ value is drastically the same as $\mathscr{R}\{x(t)\}$. $\mathscr{R}\{x(t)\}$ indicates that a random fluctution exists from cycles to cycles, yet it is two orders of magnitude smaller than the mean value $\mathscr{P}\{x(t)\}$; it is obviously second-order cyclostationary since squaring it produces periodic components.

Let's consider x(t) after removing the first order cyclostationarity part.To mesure the mean interaction between two values of the signal spaced apart by time-lag τ around time instant t, respectively $x(t+\tau/2)$ and $x(t-\tau/2)$,we use the *autocorrelation function* :

$$\begin{aligned} R_x(t,\tau) &= \mathbb{E}\{x(t+nT-\tau/2)x^*(t+nT+\tau/2)\} = \mathscr{P}\{x(t+\tau/2)x(t-\tau/2)\} \\ &= \sum_{\alpha\in\mathscr{A}} \mathscr{P}_0\{x(t+\tau/2)x(t-\tau/2).e^{-j2\pi\alpha t}\}.e^{j2\pi\alpha t} \\ &= \sum_{\alpha\in\mathscr{A}} R_x^\alpha(\tau).e^{j2\pi\alpha t} \end{aligned} \tag{7}$$

Where $R_x^\alpha(\tau)$ is the Fourier series of $R_x(t,\tau)$ so-called *cyclic autocorrelation function* . The *autocorrelation function* reveals the repetitive bursts of energy , that characterizes the presence of a periodic mechanism. In

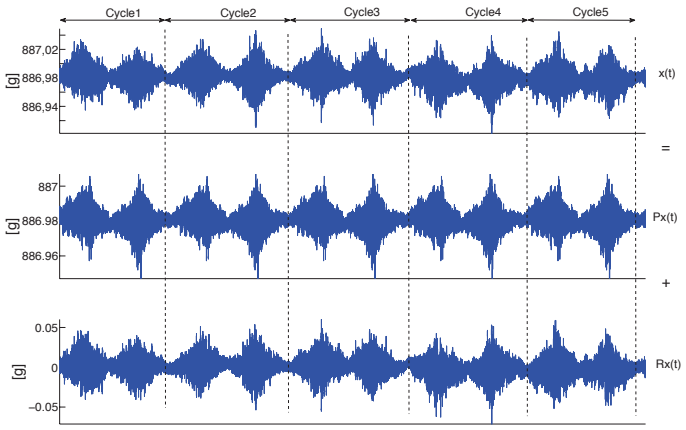

Figure 12: Decomposition of the signal into deterministic and random parts

the particular case of $\tau = 0$, $R_x(t,0)$ is *the mean instantaneous power* and $R_x^\alpha(0)$ is the *cyclic power* .The *mean instantaneous power* $R_x(t,0)$ provides a global vision on how the energy of a signal is flowing with respect to time.

4.5 Mathematical model for cyclic analysis

The cyclostationarity results from coupling between periodic phenomenon and another stationary but random ones. A model for the nature of modulation is given as follow :

$$x(t) = \sum_k [B_k + A_{2k}(t)] cos(2\pi k f_0 t) + b(t) \tag{8}$$

Where B_k is a constant since it depends pratically on the specimen material and on the mecanique stress, and f_0 is the sliding frequency. The randomness is given by the amplitude $A_k(t) \sim \mathcal{N}(0, \sigma_A^2)$ which is $\ll 1$. We assume that this amplitude is linked to the specimen damage state. The parameter $b(t) \sim \mathcal{N}(0, \sigma_b^2)$ is independent and identically distributed noise. Equation Eq.8 can be decomposed as follow :

$$x(t) = \sum_k B_k cos(2\pi k f_0 t) + \sum_k A_k(t) cos(2\pi k f_0 t) + b(t) \tag{9}$$

- The first order cyclostationarity part of $x(t)$ is represented by $\sum_k B_k cos(2\pi k f_0 t)$.
- Whereas $\sum_k A_k(t) cos(2\pi k f_0 t) + b(t)$ represents the second order cyclostationary part.

To simplify equations, let's consider $x(t) = A(t) cos(2\pi f_0 t) + b(t)$ after removing the first order cyclostationarity part. The instantaneous correlation of $x(t)$,is as follow :

$$\begin{aligned} R_x(t,\tau) &= \mathbb{E}\{x(t-\tau/2)x^*(t+\tau/2)\} \\ &= \mathbb{E}\{A(t+\tau/2)A(t-\tau/2)\}\frac{1}{2}\Big(cos(2\pi f_0(2t)) + cos(2\pi f_0 \tau)\Big) \\ &\quad +\mathbb{E}\{Ax(t+\tau/2)b(t+\tau/2)\}cos(2\pi f_0(t+\tau/2)) \\ &\quad +\mathbb{E}\{A(t-\tau/2)b(t-\tau/2)\}cos(2\pi f_0(t-\tau/2)) \\ &\quad +\mathbb{E}\{b(t+\tau/2)b(t-\tau/2)\} \end{aligned} \tag{10}$$

When $A(t)$ and $b(t)$ are uncorrelated $\mathbb{E}\{A(t)b(t)\} = 0$. With $\sigma_A^2\delta(\tau) = \mathbb{E}\{A(t+\tau/2)A(t-\tau/2)\}$ and $\sigma_b^2\delta(\tau) = \mathbb{E}\{b(t+\tau/2)b(t-\tau/2)\}$ we obtain :

$$R_x(t,\tau) = \frac{1}{2}\sigma_A^2\delta(\tau)cos(2\pi(2f_0)t)) + \frac{1}{2}\sigma_A^2\delta(\tau)cos(2\pi f_0\tau) + \sigma_b^2\delta(\tau) \quad (11)$$

This shows that $R_x(t,\tau)$ is periodic at $1/2f_0$ and $1/f_0$. The cyclic-correlation is given as follows :

$$\begin{aligned} R_x^\alpha(\tau) &= \frac{1}{4}.\sigma_A^2\delta(\tau)\delta(\alpha - 2f_0) + \frac{1}{4}\sigma_A^2\delta(\tau).\delta(\alpha + 2f_0) \\ &+\Big(\frac{1}{2}\sigma_A^2\delta(\tau)cos(2\pi f_0\tau) + \sigma_b^2\delta(\tau)\Big)\delta(\alpha) \end{aligned} \quad (12)$$

$R_x^\alpha(\tau)$ is nonzero for $\alpha = \pm 2f_0$ and 0.

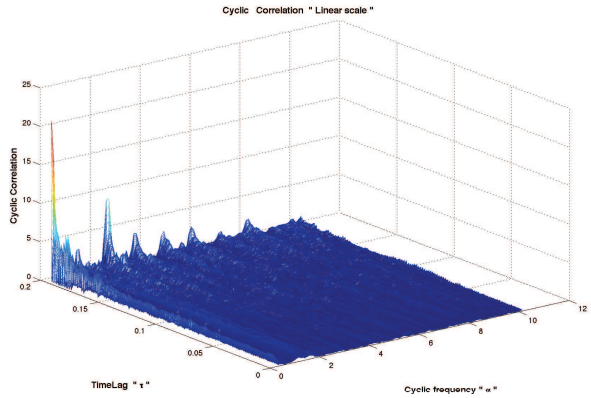

Figure 13: Cyclic correlation applied on residual signal $\mathscr{R}\{x(t)\}$ estimated by synchrone analysis

The Figure (13) displays the cyclic correlation of the vibration signal. It is seen that the cyclic-correlation is essentially dominated by a distribution of spectral points below $f_0 = 1.2$ Hz that are spaced apart by increments of $1.2Hz$ along the alpha cyclic frequency axis. The frequency $f_0 = 1.2$ hz correspond to the engine frequency. We can see that the highest energy appears in the cyclic frequency of $2f_0 = 2 * 1,2Hz$ corresponding to the round-trip frequency. As discussed before, this is the signature of second-order cyclostationary components.

To reveal certain types of hidden periodicities it is necessary to scrutinize how *the mean instantaneous power* is distributed in frequency domain. The *spectral correlation density* $SC_x^\alpha(f)$ allows to do this observation :

$$R_x(t,\tau) = \sum_{\alpha\in\mathscr{A}} R_x^\alpha(\tau).e^{j2\pi\alpha t} = \sum_{\alpha\in\mathscr{A}} SC_x^\alpha(f).e^{j2\pi ft}.e^{j2\pi\alpha t} \quad (13)$$

$SC_x^\alpha(f)$ is a density of correlation of two spectral components (f_1 and f_2) spaced apart by α around the central frequency f ie $f = (f_1 + f_2)/2$ and $\alpha = f_2 - f_1$.

The spectral correlation density is given as follows :

$$\begin{aligned} S_x^\alpha(f) &= \frac{1}{4}\sigma_A^2.\delta(\alpha - 2f_0) + \frac{1}{4}\sigma_A^2.\delta(\alpha + 2f_0) \\ &+\frac{1}{4}\sigma_A^2\delta(f + f_0)\delta(\alpha) + \frac{1}{4}\sigma_A^2\delta(f - f_0)\delta(\alpha) + \sigma_b^2\delta(\alpha) \end{aligned} \quad (14)$$

By generalizing to the model defined in Eq9 we get :

$$\begin{aligned} S_x^\alpha(f) &= \sum_k \frac{1}{4}\sigma_{A_k}^2.\delta(\alpha - 2kf_0) + \frac{1}{4}\sigma_{A_k}^2.\delta(\alpha + 2kf_0) \\ &+\frac{1}{4}\sigma_{A_k}^2\delta(f + kf_0)\delta(\alpha) + \frac{1}{4}\sigma_{A_k}^2\delta(f - kf_0)\delta(\alpha) + \sigma_{b_k}^2\delta(\alpha) \end{aligned} \tag{15}$$

$S_x^\alpha(f)$ is nonzero for $\alpha = \pm 2f_0$ and 0. The fundamental cyclic frequencies are $\pm 2f_0$, the harmonics are $\{\pm 2kf_0, k = 2, 3, ...\}$.

Let us consider $x_{\Delta f}(t, f)$, the filtered version of signal $x(t)$ through a frequency band of width Δf centred on frequency f. The $\mathscr{P}$-operator applied to $x_{\Delta f}(t, f)$ describes how the energy is flowing with respect to both time and frequency. The obtained quantity $P_x(t, f, \Delta f)$ is a time-frequency spectrum named *instantaneous power spectrum* :

$$\begin{aligned} P_x(t, f, \Delta f) &= \mathscr{P}\{|x_{\Delta f}(t, f)|^2\} \\ &= \sum_{\alpha \in \mathscr{A}} \mathscr{P}_0\{|x_{\Delta f}(t, f)|^2 .e^{-j2\pi\alpha t}\}.e^{j2\pi\alpha t} \\ &= \sum_{\alpha \in \mathscr{A}} P_x^\alpha(f; \Delta f).e^{j2\pi\alpha t} \end{aligned} \tag{16}$$

The Fourier coefficient $P_x^\alpha(f; \Delta f)$ quantifies the intensity of such hidden periodicities, it is the *cyclic modulation spectrum* . In [7], it has been shown that :

$$\int_{\Delta f} SC_x^\alpha(f).df = P_x^\alpha(f; \Delta f) = \mathscr{P}_0\{|x_{\Delta f}(t, f)|^2 .e^{-j2\pi\alpha t}\} \tag{17}$$

So the random part $\mathscr{R}\{x(t)\}$ may be estimated in filtering the signal $x(t)$ through a specific frequency band of width Δf centred on a specific frequency f:

$$\mathscr{R}\{x(t)\} = x_{\Delta f}(t, f) \tag{18}$$

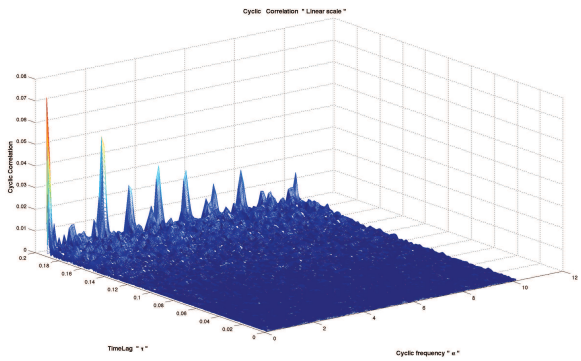

Figure 14: Cyclic correlation applied on residual signal $\mathscr{R}\{x(t)\}$ estimated by filtering of $x(t)$.

We can choose the optimal set $\{\Delta f; f\}$ using the Kurtogram [8] or by choosing f corresponding to high frequencies, around a resonant frequency in order to take advantage of the treadmill resonance, with Δf wide band. In our case we have chosen the second way with $\{\Delta f; f\} = [22KHz : 23KHz, 22, 5KHz]$ with $22, 5KHz$ a resonant frequency.

As illustred in the figure (15), the deterministic part of the resulting signal $x_{\Delta f}(t,f)$ is nil and its spectrum $\mathscr{P}_0\{x_{\Delta f}(t,f).e^{-j2\pi\alpha t}\}$ presents no cyclic frequencies. However, the spectrum $\mathscr{P}_0\{|x_{\Delta f}(t,f)|^2.e^{-j2\pi\alpha t}\}$ reveals cyclics frequencies α related to the hidden periodicities of the vibration signal $x(t)$. Zooming of $\mathscr{P}_0\{|x_{\Delta f}(t,f)|^2.e^{-j2\pi\alpha t}\}$ at low frequencies, clatity the cyclic frquency $\alpha = 1,2Hz$ and its harmoniques. We can also remark that the signal power is essentially distributed in the cyclic frequency $2,4Hz$ and on its harmoniques : The vibration signal $x(t)$ contains a hidden periodicity at the cyclic freqeuncy $\alpha = 2,4Hz$ which macthes the round-trip frequency.

The figure (14) displays the cyclic correlation of the random noise $\mathscr{R}\{x(t)\} = x_{\Delta f}(t,f)$. In comparison to the cyclic correlation displayed in the figure (13), we notice that the energy of the frequency $2f_0 = 2,4Hz$ and its harmoniques appear significantly in relation to the frequency $f_0 = 1,2Hz$, but with a lowest value : 10g for the first estimation showen in figure (13) and 0.05g for the second estimation showen in figure(14).

These observations show that the signal $x_{\Delta f}(t,f)$ is purely cyclostationary at order 2, with the cyclic frequency $\alpha = 2f_0 = 2,4Hz$, and confirms the mathematical model that we suggest.

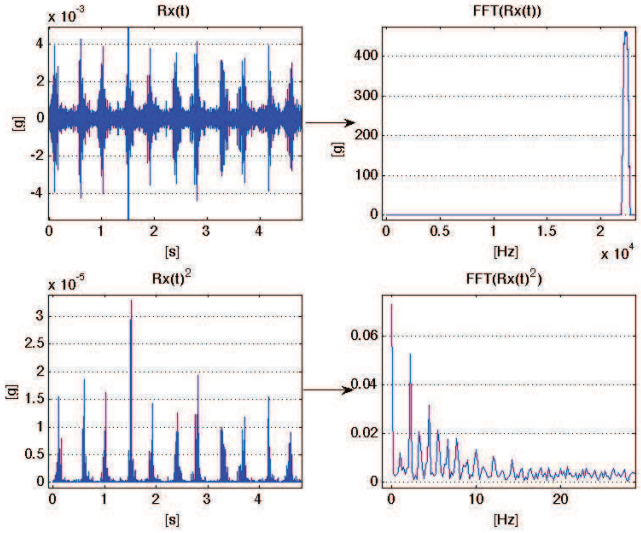

Figure 15: Comparison between $\mathscr{P}_0\{x_{\Delta f}(t,f).e^{-j2\pi\alpha t}\}$ and $\mathscr{P}_0\{|x_{\Delta f}(t,f)|^2.e^{-j2\pi\alpha t}\}$

5 Identification of the fatigue

5.1 Mechanical solicitation description

Specimens are subjected to a cyclic sinusoidale mechanical sollicitation. Indeed, the fatigue phenomenon is characterized by commencing microcrack apparition on the surface. These microcracks increase in the surface and spread until the fracture occurs. They macrocrack spread through the material, at first slowly and the pace become more and more quickly until breaking [9]. Our study is carried out in the framework of plastic fatigue damage, and we applied stresses superiors to the elastic limit Rp at $0,2\%$ of 220 Mpa : 550 Mpa and 350 Mpa. For stress of 350 Mpa, the nunmber of cycles to damage N_f is above 10^6, which corresponds to high cycle fatigue. For stress of 550 Mpa, N_f is below 10^6, which corresponds to low cycle fatigue.

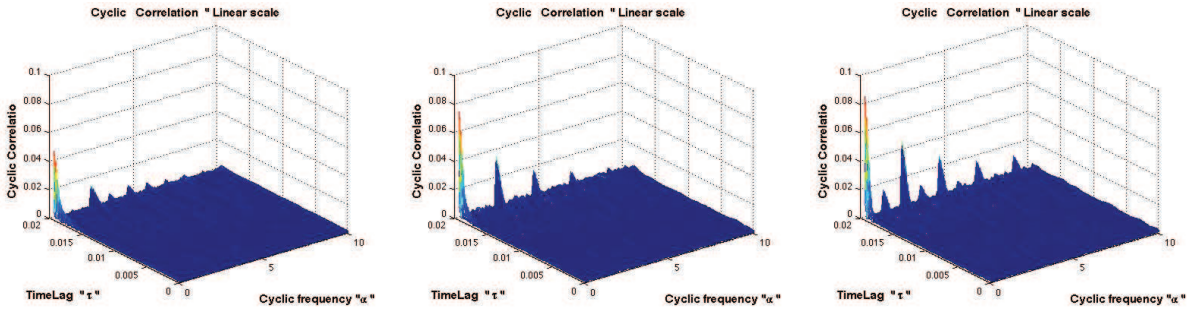

(a) In the starting (b) During the test (c) At the breaking

Figure 16: Cyclic correlation during the test

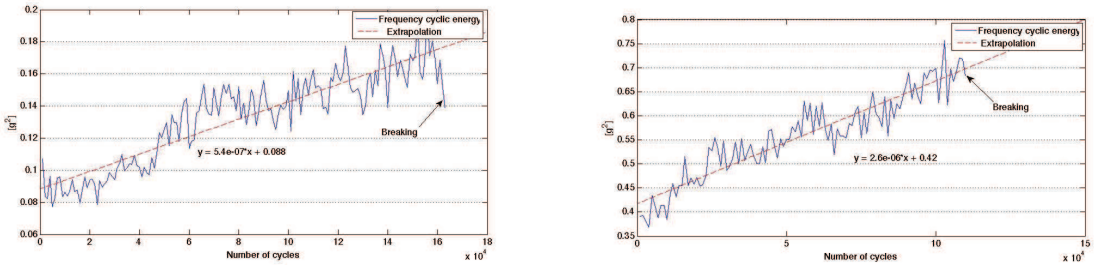

(a) test specimen1 (b) test specimen2

Figure 17: Tracking of the frequency energy over the number of cycles

5.2 Low cycle fatigue : Tracking of cyclic frequency energy

At 550 Mpa stress, we tracked the energy of cyclic frequency. As illustrated in figure(16), we observed that the energy of cyclic frequency increases with the damage of the specimen until the breaking. Figure(17) shows the tracking of the cyclic energy for two identical test specimen at same stress. At the beginning of the test we noticed a significant cyclic frequency energy which increases linearly with respect to the number of cycle before breaking. Although we see this trend, for each specimen, we observe neither the same slope nor the same maximum value of the cyclic energy at the breaking. For example for the specimen1 we have a slope of $5,4.10^{-7}$ for a maximum value of cyclic energy of 0,2 g^2 whereas for the specimen2 we have a slope of $2,6.10^{-6}$ for a maximum value of cyclic energy of 0,75 g^2. These observations show that it is difficult to define a cyclic energy threshold for the detection of the rupture. Indeed the energy dispersion of a specimen to another are very important. Whatever the cyclic energy increases with damage.

5.3 High cycle fatigue : Tracking of energy cyclic frequency

At 350 Mpa stress, we tracked the energy of cyclic frequency.As illustrated in figure(18) we note that at the beginning of the fatigue tests, cyclic energy is 0.05 g^2 and remains constant over 250000 cycles, from which it increases up to 885000 cycles. From 885000 cycles the cyclic energy decreases immediatly and remains constant throughout the test. After 1 month of operation (2.10^6 cycles), the specimen was not broken. In the field of high cycle fatigue, at the beginning of the cyclic test the energy is constant and increases after a high number of cycle.

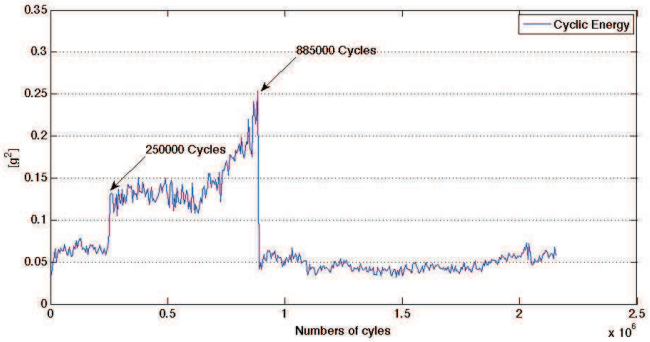

Figure 18: Tracking of the frequency energy over the number of cycles

5.4 Origin of the Cyclostationarity at the order 2 : the strain hardening effect

During deformation at room temperature, the atomic bonds deform elastically with the stress. In this case, the metal returns to its original shape when we remove the stress : its the elastic deformation. If the stress is kept beyond the elastic limit, it follows plastic deformation resulting from the shift of part of the crystal relative to another, according to certain inter-reticular distances. This type of shift is favored by the formation, multiplication and movement of line defects in the crystal called mobile ”dislocations”. Dislocation motion is not reversible, the metal does not resume its original shape when you remove the constraint. The increasing number of dislocations produced during plastic deformation and their interaction with each other ,leads to reduced mobility : it is the phenomenon of strain hardening that result in a hardening of the metal [10].

Several studies have shown that in the case of austenitic stainless steel, strain hardening causes a change in crystal structure [11] [12]. Indeed under the work hardening, the metastable austenite was transformed to hardening martensite. Results of studies [13] and [14] showed that the volume fraction of transformed martensite increases with increasing prestrain. Indeed the work hardening of steels increased with increasing martensite content and the transformed martensite in the microstructure remarkably affects the deformation behavior of the steel.

Studies of materials science have clearly shown that stainless steel subjected to strain hardening suffered a molecular transformation of austenite to hardening martensite and that it becomes unstable. We think and put the hypothesis that this unstability appears in a vibration signal as a random periodic component to the period of solicitation. The cyclostationarit to order 2 is linked to the hardening state of materials, thus to its level of damage.

6 Conclusion

The cyclic frequency energy is linked to the chemical composition of the specimen. During the damage, in the presence of hardening strain, the austenite is transformed to a hardening martensite and becomes unstable. This unstability appears in the vibration signal by a hidden random component periodic at the periode of the sollicitaion. More the material is damaged more we have martensites and most important is the cyclic frequency energy. Therefore it is possible to track the damage of a stainless steel by means of the cyclostationarity at the order 2 .

References

[1] K. Sabri, M. E. Badaoui, F. Guillet, A. Belli, G. Millet, and J. B. Morin, "Cyclostationary modeling of ground reaction force signals," *Signal Processing*, vol. 90, no. 4, pp. 1146 – 1152, 2010. lt;ce:title¿Special Section: Ethnic Music Audio Documents: From the Preservation to the Fruitionlt;/ce:title¿.

[2] W. Gardner, *Cyclostationarity in communications and signal processing*. Electrical engineering, communications and signal processing, IEEE Press, 1994.

[3] W. A. Gardner, A. Napolitano, and L. Paura, "Cyclostationarity: Half a century of research," *Signal Processing*, vol. 86, no. 4, pp. 639 – 697, 2006.

[4] J. Antoni, "Cyclostationarity by examples," *Mechanical Systems and Signal Processing*, vol. 23, no. 4, pp. 987 – 1036, 2009.

[5] J. Mercier, W. Kurz, and G. Zambelli, *Introduction à la science des matériaux*. Traité des matériaux, Presses polytechniques et universitaires romandes, 1999.

[6] C. Lemaignan, *La rupture des matériaux*. EDP Sciences, 2003.

[7] R. Randall, J. Antoni, and S. Chobssard, "The relationship between spectral correlation and envelope analysis in the diagnostics of bearing faults and other cyclostationary machine signals," *Mechanical Systems and Signal Processing*, vol. 15, no. 5, pp. 945 – 962, 2001.

[8] J. Antoni, "Fast computation of the kurtogram for the detection of transient faults," *Mechanical Systems and Signal Processing*, vol. 21, no. 1, pp. 108 – 124, 2007.

[9] B. I. S. Degallaix, *Traité des matériaux, Caractérisation expérimentale des matériaux*. Presses polytechniques et Universitaires romandes, 2007.

[10] B. Dagallier, *Manuel technique des aciers inoxydables*. Pyc-Édition, 1977.

[11] G. M. Jean Barralis, *Précis de Métallurgie: élaboration, structures-propriétés et normalisation*. 2091940178, 9782091940175, Nathan, 3 ed., 1983.

[12] P. Lacombe, B. Baroux, and G. Béranger, *Les Aciers inoxydables*. Les Éditions de Physique, 1990.

[13] A. Zare and A. Ekrami, "Effect of martensite volume fraction on work hardening behavior of triple phase (tp) steels," *Materials Science and Engineering: A*, vol. 528, no. 13â"14, pp. 4422 – 4426, 2011.

[14] Z. yu XUE, S. ZHOU, and X. cheng WEI, "Influence of pre-transformed martensite on work-hardening behavior of sus 304 metastable austenitic stainless steel," *Journal of Iron and Steel Research, International*, vol. 17, no. 3, pp. 51 – 55, 2010.